FRACTURE AND MICROSTRUCTURE OF WOOD

Stefanie E. Stanzl-Tschegg[1], Klaus Frühmann[1] and Elmar K. Tschegg[2]
[1] Institute of Physics and Materials Science and Christian Doppler Laboratory for Fundamentals of Wood Machining, BOKU - University of Natural Resources and Applied Life Sciences Vienna, Austria
[2] Institute of Solid State Physics, Vienna University of Technology, Austria

ABSTRACT

The fracture properties of wood are strongly influenced by its inhomogeneous microstructure. The relationship between structure and function with regard to damage and fracture behaviour can be only understood with a sufficiently fine level of examination. *In situ* fracture mechanical experiments were carried out in an Environmental Scanning Electron Microscope (ESEM) chamber on spruce and beech. They were performed with micro-wedge splitting specimens, and the experimental procedure is designed to allow stable crack propagation. The ESEM-mode combined with a cooling device allows examination of the specimens at a moisture content of 12% with unsputtered surfaces. By recording load-displacement curves and observing crack propagation simultaneously, a detailed image of the fracture process is possible. Besides Mode I loading, mixed mode (mode I plus II) loading could be realized by using a modified wedge splitting technique. The resulting specific fracture energies are not algebraic sums of the tensile and shear componenrts, but a coupling between the two modes.

1 INTRODUCTION

Wood is a highly anisotropic and complex material with a large variability of mechanical properties. Therefore fracturing is a complex process, which needs additional methods for its quantitative characterisation besides conventional fracture mechanical procedures. One straight-forward technique is the wedge splitting technique according to Tschegg [1], which has been developed to make possible recording of the load-displacement diagrams during the fracturing process and to determine the specific fracture energy G_f as an important material characterising parameter. Combining this technique with environmental scanning microscopy allows performing *in situ* experiments, which give more insight into the structural features and mechanisms, being responsible for the different fracture processes of wood in the sub-microscopic range. Some more recent investigations will be reported in the following. They refer to these new testing techniques as well as to results correlating measured characteristic quantitative parameters with observations of fracture processes on different levels of magnification.

2 EXPERIMENTAL METHODS

2.1 In situ cracking in an ESEM

Using an environmental scanning electron microscope (ESEM) with a cooling device makes observation of wood in moistured condition possible. Applying in addition an *in situ* deformation stage allows to perform tensile tests or fracture mechanical measurements inside the microscope under almost natural conditions. The tests are performed with two spindle-driven crossheads carrying the jaws to clamp the specimens. A load cell of 1 kN is placed between one crosshead and a jaw and is registering tensile or compressive forces. The machine is driven by a DC motor and a gear, which enables displacement rates between 0.3 μm/s up to 10 μm/s. The displacement is determined by the rotations of the motor and was 2 μm/s in this study. The used equipment allows

simultaneous detection of load-displacement curves and observation of a propagating crack. The *in situ* micro-wedge splitting device is shown in Fig. 1.

Figure 1 ESEM *in situ* wedge splitting device

In situ fracture mechanics tests were performed on spruce (*Picea abies* [L.] Karst) and beech (*Fagus sylvatica* L.) (Frühmann et al. [2]) after *in situ* tensile tests have been reported (Frühmann et al. [3]). The specimens were oriented in the TR crack propagation system (R = radial, T = tangential and L = longitudinal) where the first letter indicates the direction normal to the crack propagation direction and the second determines the direction of crack propagation. The wood samples were stored in a climate chamber (20°C and 65%MC) until equilibrium moisture content was reached before testing.

2.2 Mixed-mode Loading

In order to simulate mixed mode loading conditions, the wedge splitting technique was modified using an asymmetric wedge (Tschegg et al. [4]). The mode I and mode II parts are varied using different wedge angles. The mode II portion becomes larger, if the wedge angle is made larger. Angles of 10°, 25°, 39° and 50° were used. Crack propagation was stable in the experiments being performed in the RL system. The mode I and mode II displacements δ_I and δ_{II} were determined optically in a contact free manner and the specific fracture energy for mixed mode loading $G_{f,M}$ was determined as the sum of the mode I and mode II parts of the specific energies.

3 RESULTS AND DISCUSSION

3.1 In-situ cracking of micro-wedge splitting specimens (fracture mechanics test)

Fig. 2 shows ESEM images of loaded crack tips of spruce (2a,b) and beech (2d,e) and the load-displacement curves registered from *in situ* micro-wedge splitting experiments (Fig. 2c,f). The arrows mark positions when the corresponding images displayed in Fig. 2a,b and 2d,e were taken. The load is increasing linearly in the first phase of the experiment. The small interruptions originate from visco-elastic relaxation processes of the material when stopping the feed to record the ESEM images. Fig. 2a shows the crack tip in spruce wood at a load level of about –20 N shortly before the first step in crack propagation occurred (termed “4a” in Fig. 2c). The crack tip cut with the razor blade was located in earlywood. The crack front is widened but no

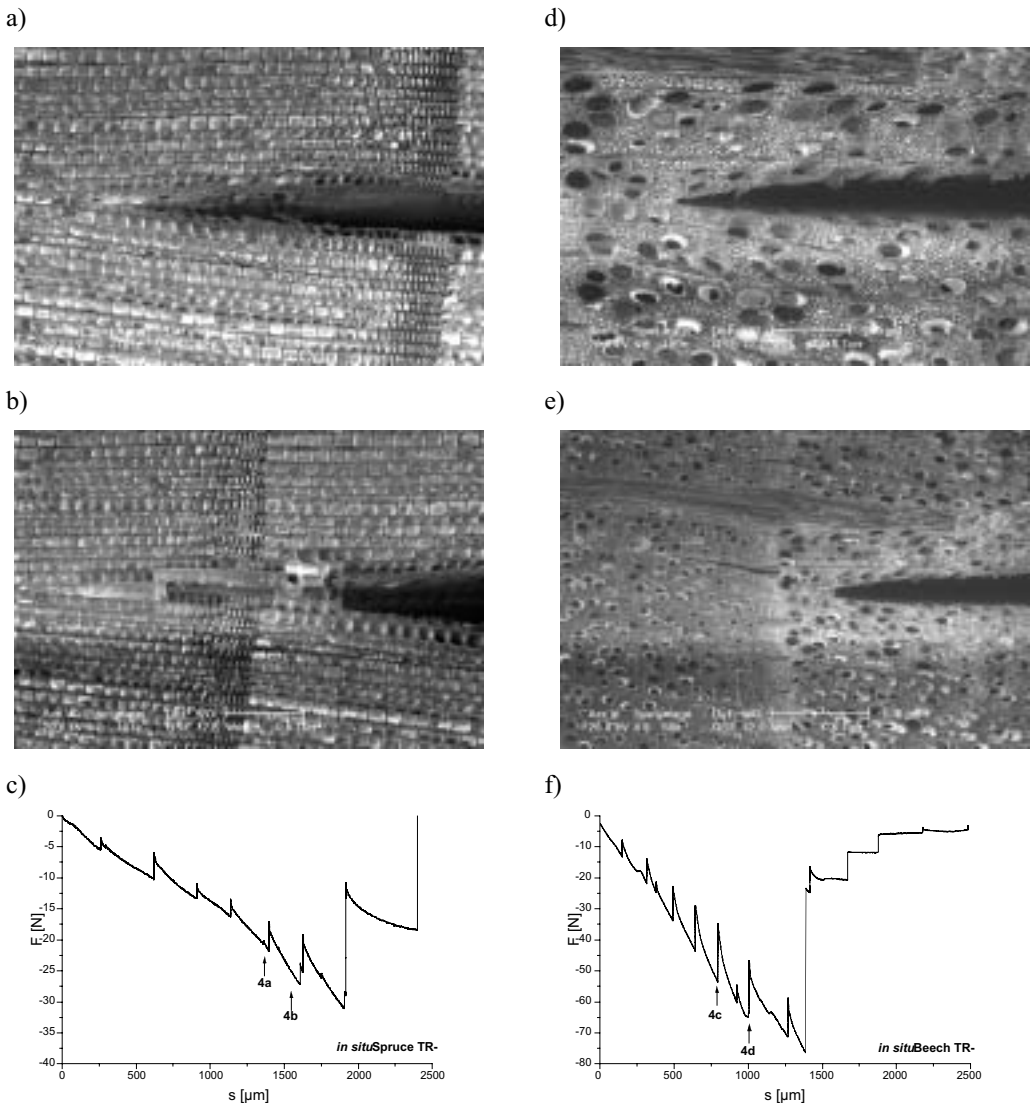

Figure 2 ESEM images of loaded crack tips and load-displacement diagrams of the *in situ* tests of spruce (a,b,c) and beech (d,e,f).

propagation took place so far. The first crack propagation event occurred at a load of –27 N, which can be seen from Fig. 2b as well as from the load drop in the load-displacement diagram (Fig. 2c, termed "4b"). The crack penetrated the first latewood layer and stopped in the earlywood zone of the next growth ring. The load increased and dropped significantly during the next step, while the crack was passing several growth rings. Analysis of the load-displacement diagrams and the corresponding ESEM images indicates some principle features of the fracture process. During the linear increase of the load, the crack length remains unchanged, and no propagation or non-linear effects such as micro-cracking or local damage are visible in the ESEM. Deviation from linearity

is accompanied by the first crack events involving several cells ahead of the crack tip. The tensile stress ahead of the crack tip deforms the cells and fractures them. The size of this developing process zone is rather small and extends only a few cell diameters. In some cases microcracks could be observed in the latewood layer, which were not connected to the main crack path (Fig. 2b). The phase of quasi-static crack initiation is followed by a bigger crack extension across several growth rings accompanied by a proportional load drop. The newly formed crack tip always stops in the earlywood zone of the material. The compound of earlywood and latewood toughens the material by combining high strength of latewood ahead of the crack tip with high elasticity of the earlywood around it. This results in a comparably higher total fracture toughness of the earlywood and favours non-stable crack propagation when penetrating latewood zones.

The load-displacement diagram of the *in situ* tested beech specimen (Fig. 2f) shows a linear elastic increase in load, interrupted only by the stops of deformation during taking the photographs and resulting visco-elastic relaxation. Figure 2d shows the crack tip at a load level of -52 N. No crack propagation from the initial state took place so far. Before passing the first local maximum (-65 N) the curve deviates slightly from linearity, which indicates beginning fracture of the material. A corresponding displacement of 1000 µm was measured. This fact can also be seen from the corresponding image (Fig. 2e), which shows a small crack penetrating the latewood zone ahead of the initial crack tip and stops in the earlywood. The load drops by 30% and increases again to the global maximum of –76N before the crack propagates throughout several growth rings and the specimen looses its load carrying capacity.

Evaluation of the recorded load displacement curves allows to determine the initial slope k_{init}, which characterises the stiffness of the material, and the critical load F_{max} indicating the maximum after the linear elastic phase, and s_{max}, which is the corresponding displacement. From $F_{max,}$ the fracture toughness K_{Ic} and the specific fracture energy G_f may be derived (Stanzl-Tschegg et al. [5]) with

$$G_f = \frac{1}{A_{lig}} \int_0^{s_{end}} F(s) \cdot ds \tag{1}$$

where A_{lig} determines the nominal area of the fracture surface.

These quantities are strongly determined by the density of wood (ρ) and cell wall (ρ_s). In Table 1, the densities and measured maximum loads are listed.

Table 1. Dependence of maximum load on relative density

	ρ	ρ_S	$(\rho/\rho_s)^{3/2}$	F_{max}	$F_{vert} \Big/ \left(\rho/\rho_S\right)^{3/2}$
	kg/m^3	kg/m^3	-	N	N
Spruce	440	1500	0.164	31.5	198.3
Beech	672	1500	0.354	66.7	222.4

Considering cellular materials, Gibson and Ashby [6] correlate the critical fracture toughness of wood loaded normal to the grain with the relative density ρ/ρ_s where ρ_s is the density of the cell wall material by the equation:

$$K_{Ic}^{a} = 1{,}8 \cdot \left(\frac{\rho}{\rho_S}\right)^{3/2} \tag{2}$$

Considering the identical geometry for all specimens of this study and the validity of Linear Elastic Fracture Mechanics (LEFM) we may assume proportionality between the critical fracture toughness K_{Ic} and the critical load F_{max} for crack initiation. Hence the ratio between critical load and density relation should be constant.

$$K_{Ic}^{a} \propto F_{\max} \propto \left(\frac{\rho}{\rho_S}\right)^{3/2} \Rightarrow F_{\max} \Big/ \left(\frac{\rho}{\rho_S}\right)^{3/2} = const. \tag{3}$$

Introducing the obtained data of the maximum load and the densities into eqn (3) results in ratios of 198,3 N for spruce and 222,4 N for beech. The relatively small difference indicates that the tests confirm the dependence of fracture toughness and relative density given in the literature for wood in the TR crack propagation system.

3.2 Mixed mode fracture energy of sprucewood

Owing to the orthotropic structure of wood (long tubular cells oriented parallel to the stem axis) considerable differences in material response to loading in different loading directions must be expected. Therefore, fracture mechanics experiments have been performed not only in the crack opening (mode I) mode and under shear loading (mode II and III) (Frühmann et al. [7], Ehart et al. [8]) but also under mixed mode (mode I + II) loading conditions on spruce and beech (Tschegg et al. [9]).

The resulting load-displacement curves verify that an increased mode II portion with increasing wedge angle is obtained. The shape of the load-displacement curves (not shown in this paper) points to a more brittle material behaviour under the mixed-mode loading condition. The mixed-mode specific fracture energies $G_{f,M}$ are plotted in Fig. 4 versus increasing wedge angles and thus increasing mode II portions. Most interesting, a minimum of the specific fracture energy at a wedge angle of 25° is obvious. This behaviour indicates a non-linear coupling of the mode I and mode II components (mode coupling) under mixed mode loading, as has been suggested by Holmberg et al. [10] using the fictitious crack model (Hillerborg et al. [11]). They showed in their simulations that a coupling between the modes means that the tensile and shear stress components of the fictitious crack zone are functions of both, the opening and the shear displacements and will lead to a minimum in the specific fracture energy for mixed mode cases.

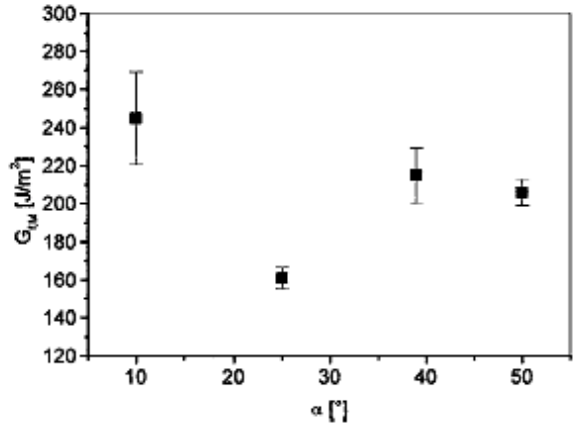

Fig. 3: Specific fracture energies for mixed mode loading in the RL system of spruce wood. Increasing of α is equivalent to an increasing portion of mode II (Tschegg et al.[9])

4 CONCLUSIONS

Combination of ESEM with a cooling device enables direct observation of the fracture processes of wood in an atmosphere with a defined moisture content. *In situ* deformation stages have been developed to perform tensile, as well as fracture mechanical tests in the ESEM. Thus the simultaneous detection of load-displacement curves and crack propagation features is possible. For both, tension as well as fracture mechanical tests, specimen shapes were developed that allow complete fracture detection until final fracturing. Experiments have been performed on spruce and beech wood in TR orientation. Information was obtained about microscopic fracture phenomena related to the structural features and their influence on mechanical as well as fracture mechanical characteristic values. Thus the mechanisms being responsible for the cracking processes can be identified on a sub-microscopic level.

Testing fracture mechanical properties in the ESEM supports the assumption that fracture of wood in the TR system can be treated by Linear Elastic Fracture Mechanics principles. The results verify the dependence of fracture toughness on relative density, as has been modelled for wood as a cellular material.

A modified wedge splitting technique has been developed in order to perform mixed mode (Mode I plus Mode II) fracture tests and determine specific fracture energies, G_f. Measurements showed that a coupling of the Mode I and Mode II components takes place. This means that tensile and shear stress components of the fictitious crack zone are functions of the crack opening as well as the shear displacements, leading to a minimum of the G_f values for mixed mode loading with high Mode I components.

REFERENCES

[1] Tschegg EK, Equipment and appropriate specimen shape for tests to measure fracture values (in German), Patent AT-390328 (1986).

[2] Frühmann K, Mode I Fracture Behaviour on the Growth Ring Scale and Cellular Level of Spruce (Picea Abies [L.] Karst.) and Beech (Fagus sylvatica L.) loaded in the TR Crack Propagation System., 653-660 Holzforschung 37 (2003).

[3] Frühmann K, Burgert I, Stanzl-Tschegg SE, Detection of the Fracture Path under Tensile Loads through in *situ* Tests in an ESEM Chamber. Holzforschung 57, 326-332(2003).

[4] Tschegg EK, Stanzl-Tschegg SE, Wedge-splitting fracture equipment for combined loading (in German), Patent AT 409038B (2002).

[5] Stanzl-Tschegg SE, Tan D.M., Tschegg EK, New splitting method for wood fracture characterization. Wood Sci. and Techn. 29, 31-50 (1995).

[6] Gibson LJ, Ashby MF, Cellular solids. Cambridge Solid State Sci. Ser. 2nd ed., Cambridge University Press, Cambridge (1997).

[7] Frühmann K, Reiterer A, Tschegg EK, Stanzl-Tschegg SE, Fracture Characteristics of Wood under Mode I, Mode II and Mode III loading. Phil. Mag. A 82, 3289-329 (2002).

[8] Ehart RJA, Stanzl-Tschegg SE, Tschegg EK, Crack face interaction and mixed mode fracture of wood composites during mode III loading. Eng. Fract. Mech. 61, 253-278 (1998).

[9] Tschegg EK, Reiterer A, Pleschberger T, Stanzl-Tschegg SE, Mixed mode fracture energy of sprucewood. J. of Mat. Sci. 36, 3531-3537 (2001).

[10] Holmberg S, Persson K, Petersson H, Nonlinear mechanical behaviour and analysis of wood and fibre materials. Comp. & Struct. 72, 459-480 (1999).

[11] Hillerborg A, Modeer M, Petersson PE, Analysis of crack formation and crack growth in concrete by means of fracture mechanics and finite elements. Cement and Concrete Research 6, 773-782 (1976).